◆ Human Brain Mapping 16:36–46(2002) ◆
DOI 10.1002/hbm.10021

Anatomically Informed Basis Functions in Multisubject Studies

Stefan Kiebel* **and Karl J. Friston**

The Wellcome Department of Imaging Neuroscience, The Institute of Neurology, London, United Kingdom

Abstract: We describe the use of anatomically informed basis functions (AIBF) in the analysis of multisubject functional imaging studies. AIBF are used to specify an anatomically informed spatial model that embodies anatomical knowledge for the statistical analysis of neuroimaging data. In a previous communication, we showed how AIBF can be used to incorporate prior anatomical constraints in single subject functional magnetic resonance image (fMRI) analyses to augment their anatomical precision. In this paper, we extend AIBF such that it can be applied to multisubject studies using fMRI or PET. The key concept is that, after spatial normalization, a canonical cortical surface can be used to generate a forward model of signal sources for all subjects. By estimating the hemodynamic signal in this canonical AIBF-space and then projecting it back into the voxel-space, one effectively extracts functional activity that is smooth, within and only within, the cortical sheet while attenuating other components unrelated to the physiological process of interest. The ensuing procedure can be considered as a highly non-stationary, anisotropic anatomically informed [de]convolution or smoothing. It is shown that this procedure offers various advantages compared to existing conventional methods for the analysis of multisubject studies, in particular it is more sensitive to underlying activations. *Hum. Brain Mapping 16:36–46, 2002.*

Key words: neuroimaging; statistical analysis; fMRI; PET; forward model; deconvolution; spatial filter

INTRODUCTION

In functional neuroimaging, multisubject studies are used to make inferences about population responses using effects observed in a group of subjects. If one employs a fixed effects analysis, the inference is about the average activation in this group. If one uses a random effects analysis, the inference is about the population from which the subjects were sampled [Friston et al., 1999]. As a special case of a fixed effects analysis, one can also use a conjunction analysis looking for activations that are common to all subjects [Worsley and Friston, 2000]. All these inferences are made using multisubject designs. One problem, when measuring hemodynamic responses in different subjects is finding a suitable transformation that projects the individuals' functional and structural data into the same anatomical space. In most neuroimaging studies, this reference space is the Talairach- [Talairach and Tournoux, 1988] or the so-called MNI-space [Collins et al., 1994]. The precision of these spatial normalization procedures is controlled by the constraints on the transformations employed e.g., by parameterizing the transformations in terms of a discrete cosine set [Ashburner and Friston, 1999]. These constraints are based

*Correspondence to: Stefan Kiebel, Functional Imaging Laboratory, Wellcome Dept. of Imaging Neuroscience, 12 Queen Square, WC1N 3BG London, UK. E-mail: skiebel@fil.ion.ucl.ac.uk
Received for publication 25 May 2001; accepted 29 October 2001

on the observation that there is no one to one mapping between two structural images and even if there was, functional areas are not located in exact relation to structural landmarks e.g., to the sulcal pattern [Amunts et al., 1999]. Therefore most normalization procedures use a rather smooth transformation.

Voxel-based methods for the analysis of functional neuroimaging data rely on the assumption that, after spatial transformation (realignment and normalization), all voxels are not only in the same anatomical reference space, but that activations over subjects are expressed in the same location. Given the functional anatomical variability across subjects, however, it is unlikely that one voxel will evidence activation in all subjects. Although any individuals' activations will fall roughly into the same region, there will be some spatial discrepancy (in the order of mm) among activations. In this situation, the usual approach is to convolve the functional data, after spatial normalization, with a stationary lowpass kernel to smear the activations together and ensure evidence of a common activation by increasing their spatial overlap. This overlap can then be detected using statistical parametric mapping (SPM). In short, resolution is traded for sensitivity. The question of optimum filter width is addressed implicitly in formal approaches to detect activations, using scale-space searches [Poline and Mazoyer, 1994] based on the theory of Gaussian random fields [Worsley et al., 1996b]. Most conventional analyses of neuroimaging data use a stationary 3D spatial lowpass filter. These filters are optimal for detecting activations that conform to the size and shape of the filter kernel. Given the underlying neuroanatomy, however, such stationary filters are almost certainly not the best in terms of sensitivity to real activations.

In this study, we resolve the problem of anatomical variability in a different way by using a non-stationary filter kernel. The basic assumption is that any activation is located within the cortical grey matter sheet. Anatomical variability can now be decomposed into two components. The first is tangential to the grey matter sheet and the second is orthogonal to the sheet. Intersubject variability will disperse the signal tangentially or within the sheet, because much of the orthogonal variability will have been removed by registering the cortical sheets during spatial normalization. The appropriate smoothing filter should therefore comprise some non-stationary kernel that, according to the matched filter theorem, conforms to the cortical sheet (i.e., has different widths in the directions tangential and orthogonal to the cortical sheet). Figure 1 shows

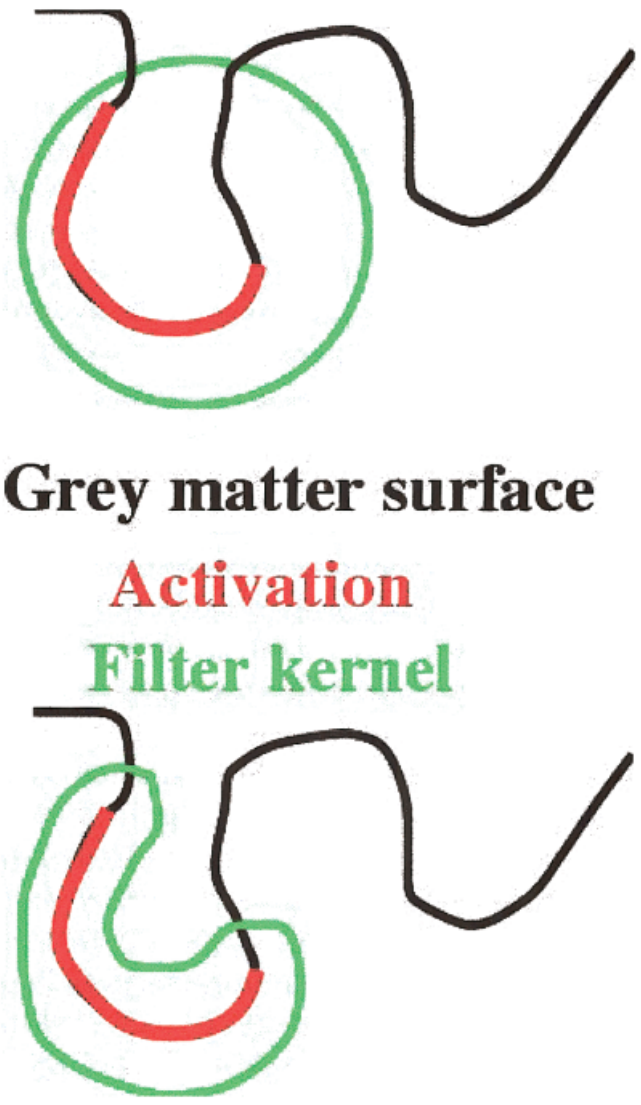

Figure 1.
Concept of anatomically informed smoothing in 2D. **Top:** Conventional stationary and spherical smoothing filter. **Bottom:** Anatomically informed variable (non-stationary) smoothing kernel.

the outline of a conventional smoothing kernel and the shape of an anatomically informed filter kernel. Given activations that arise in the cortical sheet are less dispersed in the direction orthogonal to the sheet, it is evident that the anatomically informed kernel will enhance sensitivity to these activations. It does this by taking a weighted average of voxel intensities selectively from activated locations. In contrast, the spherical filter samples a large number of non-activated locations. What follows can be seen as a simple technique to construct and apply a non-stationary, anatomically informed filter. This filter is specified by a

convolution matrix P, where the kernels constitute the rows of P.

In this study we use anatomically informed basis functions (AIBF) [Kiebel et al., 2000] to specify a spatially variable filter matrix for multisubject neuroimaging data. There are two key issues. The first is that we use a canonical surface, that models a representative cortical sheet, to generate the *same* spatially variable filter for all subjects. The second is that by explicitly specifying one smoothing kernel for each voxel, one can specify not only a smoothing matrix, but also a spatially variable deconvolution matrix that removes the effect of unwanted signal dispersion due to the effective point spread function. This is possible because we are using an explicit forward model for the spatial distribution of signal sources. Once the parameters of that model have been identified by solving the inverse problem, the forward model can be used to generate the data that would have been observed in the absence of any point spread function.

After filtering the data with the AIBF [de]convolution matrices, one can proceed with conventional analysis in the temporal domain. Here, we use statistical parametric mapping (SPM99), but any uni- or multivariate voxel- or surface-based method could be used.

We describe the theoretical background to the analysis of multisubject data with AIBF. The method is then applied to two data sets. The first is a multisubject PET and the second is a multisubject fMRI data set. Using these empirical studies, we demonstrate the advantages and potential pitfalls of AIBF.

THEORY

This section describes the generation of an anatomically informed forward model used to implement a spatially variable convolution that conforms to the cortical surface. The description is divided into three parts. First, we will outline the method of anatomically informed basis functions. Second, we specify the model and show how its parameters are estimated. Finally, we describe how these estimated parameters are projected back into image space to give a nonstationary [de]convolution.

Assuming that all activations are distributed within the cortical surface, we require a spatial model that *matches* these activation patterns. We use a linear model that attempts to explain all observed voxel intensities within a single functional image by a linear combination of smooth basis functions following the cortical surface. Such basis functions can be of any shape provided that they model smooth voxel intensity distributions tangential to the cortical surface. In this study, we use Gaussian basis functions with local support, but one could also use a discrete cosine transform set [Kiebel, 2001]. By repeatedly fitting this model to each functional image in a time-series, we estimate a spatiotemporal parameter matrix comprising one spatial parameter vector for each image. This estimated parameter matrix can then be projected back into voxel-space. The procedure of estimating parameters of the AIBF model and their subsequent back-projection is formally identical to, and can be described in terms of, a spatially variable [de]convolution.

One basic assumption we make is about separability in the spatial and temporal domain. With this assumption one can specify the same spatial model for each image before analyzing the ensuing time-series.

Basis function specification

The following is described in detail in Kiebel et al. [2000], but is briefly reprised here for completeness. Given a surface reconstruction of a human brain $S = (V, F)$, where V is a $N_V \times 3$ matrix of vertex coordinates and F is a $N_F \times 3$ matrix of vertex indices, the graph S approximates the grey matter surface. In the following, V will be referred to as a vertex-matrix and F as a face-matrix.

Let $S_F = (V_F, F)$ be the flattened version of S, i.e., S has been projected to a plane, e.g., Fischl et al. [1999]. Given a 2D coordinate system on S_F, the Gaussian basis function b_F^j with its centre at coordinates (x_j, y_j) is defined by

$$b_F^j(x, y) = c_1 \exp\left(\frac{-((x - x_j)^2 + (y - y_j)^2)}{2w^2}\right) \quad (1)$$

where c_1 is a constant and w is the (user-specified) width of the basis function in the x- and y-directions. The hexagonal pattern of the centres of the basis functions are defined by induction, i.e., given that (x_j, y_j) is the centre of b_F^j, then the centers of its six neighbor basis functions are $(x + d/2, y + d_o)$, $(x + d, y)$, $(x + d/2, y - d_o)$, $(x - d/2, y - d_o)$, $(x - d, y)$, $(x - d/2, y + d_o)$, where d is a fixed distance between centres and $d_o = \sin(60^0)\mathrm{d}$. The basis functions are sampled discretely at vertex positions.

The next step is to project the basis function b_F^j to the folded surface S. This is effected by a coordinate exchange from V_F to V resulting in basis function b_G^j. The final step is to project b_G^j to the space in which images

were acquired (measurement space). To do this, an operator g is defined, that integrates, over each voxel k, the surface of a given basis function b^j_G multiplied by the height of the basis function, i.e., g returns the integral of each basis function in folded vertex-space encompassed by the voxel. We assume that the activity distribution on a given face is a linear function of activity at the three vertices of this face. Then a $N_K \times N_V$ matrix G can be defined, where N_K is the number of voxels. The jth column of G specifies the observed activity in voxel-space produced by unit activity at vertex j.

The matrix-vector multiplication Gb^j_G transforms the basis function b^j_G in vertex-space to b^j_Y ($b^j_Y = b^j_{Y1},\ldots, b^j_{Y_{N_k}}$). This is the jth AIBF in voxel-space.

Model specification

Let A_G be a $N_V \times N_p$-matrix, where column j of A_G is the basis function b^j_G in vertex-space, i.e., $A_G = [b^1_G|\ldots|b^{Np}_G]$ and N_p is the number of basis functions. To project these onto voxel space we multiply by G to give $A = GA_G$.

To model effects of any point spread function (PSF) due to the measurement process (e.g., PET), let L_I be a $N_K \times N_K$ convolution matrix. Let L_E be a $N_K \times N_K$ convolution matrix that models any additional exogenous smoothing applied to data and model. Applying L_E will allow us to capture activations that are not very close to the cortical sheet, but follow the shape of the cortical sheet over some short distance. The width of L_E controls the width of the smoothing of the manifold containing the basis functions. In terms of the implicit non-stationary deconvolution described in the introduction, L_E specifies how much anatomical variability is deconvolved out of the direction orthogonal to the surface S.

Finally, we assemble all the smoothed basis functions into a matrix

$$A_L = L_E L_I A \tag{2}$$

The general linear model for the data is simply:

$$L_E Y^i = A_L \beta^i + L_E \epsilon \tag{3}$$

where Y^i is a N_K-dimensional observation vector in voxel-space (the ith functional image), β^i is a N_p-dimensional parameter vector and ϵ is a N_K-dimensional error vector.

Fitting the model for one time point

The model parameters in equation (3) are estimated in a least-squares sense with

$$\hat{\beta} = (A_L^T A_L + \lambda W^T W)^{-1} A_L^T L_E Y^i \tag{4}$$

where W is an appropriate weighting matrix and λ is a regularization factor. We obtain good results by using a simple zeroth-order regularization, i.e., $W = I_{Np}$, the identity matrix of rank N_p. The regularization factor λ can be computed using results from Press et al. [1992]

$$\lambda = \frac{\text{trace}(A_L^T A_L)}{\text{trace}(W^T W)} \tag{5}$$

or by using a more sophisticated method like restricted maximum likelihood (ReML), which can be implemented by the EM-algorithm [Dempster et al., 1977].

Temporal domain

Given a series of functional observations $Y = [Y^1|\ldots|Y^{N_Y}]$, we estimate for each Y^i a parameter vector $\hat{\beta}^i$ using equation (4) and assemble a $(N_Y \times N_p)$ estimated parameter matrix

$$\begin{aligned} B^T &= [\hat{\beta}^1| \ldots |\hat{\beta}^{N_Y}] \\ &= (A_L^T A_L + \lambda W^T W)^{-1} A_L^T L_E [Y^1| \ldots |Y^{N_Y}] \end{aligned} \tag{6}$$

that represents the estimate of functional observations, in the space of anatomically informed basis functions. The estimated signal in voxel-space, subject to convolution by $L_E L_I$, is given by

$$B_L = BA_L^T = BA^T L_I^T L_E^T \tag{7}$$

Similarly, if $L_E \neq I_{NK}$, one can project the estimated parameters into voxel-space subject to convolution with L_I (only) by

$$B_{L_I} = BA^T L_I^T \tag{8}$$

The estimated signal in the voxel-space, but without any convolution (extrinsic or intrinsic) by $L_E L_I$ is

$$B_A = BA^T \tag{9}$$

By omitting L_E or $L_E L_I$ one is effectively deconvolving the data (see below).

Equations (7–9) can be expressed in an alternative form. By substituting equation (6) in equation (7),

$$B_L = [Y_1| \ldots |Y_{N_Y}]^T L_E^T A_L (A_L^T A_L + \lambda W^T W)^{-T} A_L^T \quad (10)$$

Let

$$P_{AL} = L_E^T A_L (A_L^T A_L + \lambda W^T W)^{-T} A_L^T \quad (11)$$

such that

$$B_L = [Y_1| \ldots |Y_{N_Y}]^T P_{AL} \quad (12)$$

P_{AL} is a $N_K \times N_K$ matrix that projects the data convolved with L_E onto the estimated response to give B_L. P_{AL} represents an anatomically informed spatially-variable filter matrix, where each column k of P_{AL} encodes the kernel at voxel k. The projection matrix that represents an anatomically informed deconvolution of the data in equation (9) is given by

$$P_A = L_E^T A_L (A_L^T A_L + \lambda W^T W)^{-T} A^T \quad (13)$$

P_A effectively performs a least squares deconvolution of the data orthogonal to the cortical surface while preserving smoothness within the sheet. These projector matrices give us natural tools to make inferences about the activations in any space that the basis functions encompass. This allows us to infer not only about the fitted effects in A_L-space given by equation (7) but also in the A-space (equation 9), i.e., a space void of convolution with L_E or L_I. Projection to A-space (equation 13) corresponds to an anatomically informed least squares deconvolution of the point spread function ($L_E L_I$) out of the data.

The Canonical Surface

AIBF can be applied to any neuroimaging data (fMRI, PET, SPECT). The application of AIBF to single subject data has been described in Kiebel et al. [2000]. The applicability to multisubject data, as presented here, is based on the convolution of the model with a lowpass filter L_E and the implicit deconvolution that obtains after fitting the model (equation 3). This approach rests on another assumption; that the surface used for generating the AIBFs is a close approximation to the spatially normalized surface of each subject. The technique is robust to violations of this assumption, because effects of errors in the normalization or anatomical variability among subjects are deliberately attenuated by the lowpass filter L_E.

Summary of the method

Two general linear models are fitted to the data, the first (AIBF as described above) is in the spatial domain and the second is in the temporal domain. The temporal component is implemented using SPM99 so that the only part of the AIBF-analysis that differs from a conventional analysis (e.g., SPM99) is the AIBF source reconstruction. This involves a choice for the smoothing filter L_E applied to the realigned and normalized functional image-series. In a conventional analysis, the spatial smoothing filter is a stationary lowpass filter of a user-specified width. With AIBF, one implements a non-stationary kernel, which takes the underlying neuroanatomy into account. This process is described schematically in Figure 2. In single subject studies, one generally uses the individual's reconstructed grey matter surface as anatomical constraints. For multi-subject studies, we propose using a canonical surface to generate the AIBFs. After choosing a set of basis functions, one specifies the width of the stationary filters L_I and L_E, where L_I emulates the point spread function of the acquisition system and L_E reflects the accuracy of the anatomical model. In a single subject study, L_E can be very small, because the individual's reconstructed surface should be a fairly accurate estimate of the true grey matter surface. In multisubject studies, L_E should be larger to render the model robust with respect to normalization errors and anatomical variability among subjects. In the following analysis of PET and fMRI data, we employ the smoothing and deconvolution scheme as summarized in equation (13).

PET data

The data were obtained from five subjects scanned 12 times (every 8 min) while performing one of two verbal tasks. Scans were acquired with a CTI PET camera (953B, CTI, Knoxville, TN). ^{15}O was administered intravenously as radiolabeled water infused over 2 min. Total counts per voxel during the build-up phase of radioactivity served as an estimate of regional cerebral blood flow (rCBF). One task involved repeating a letter presented aurally, at one per two seconds (word shadowing). The other was a paced verbal fluency task, where the subjects responded

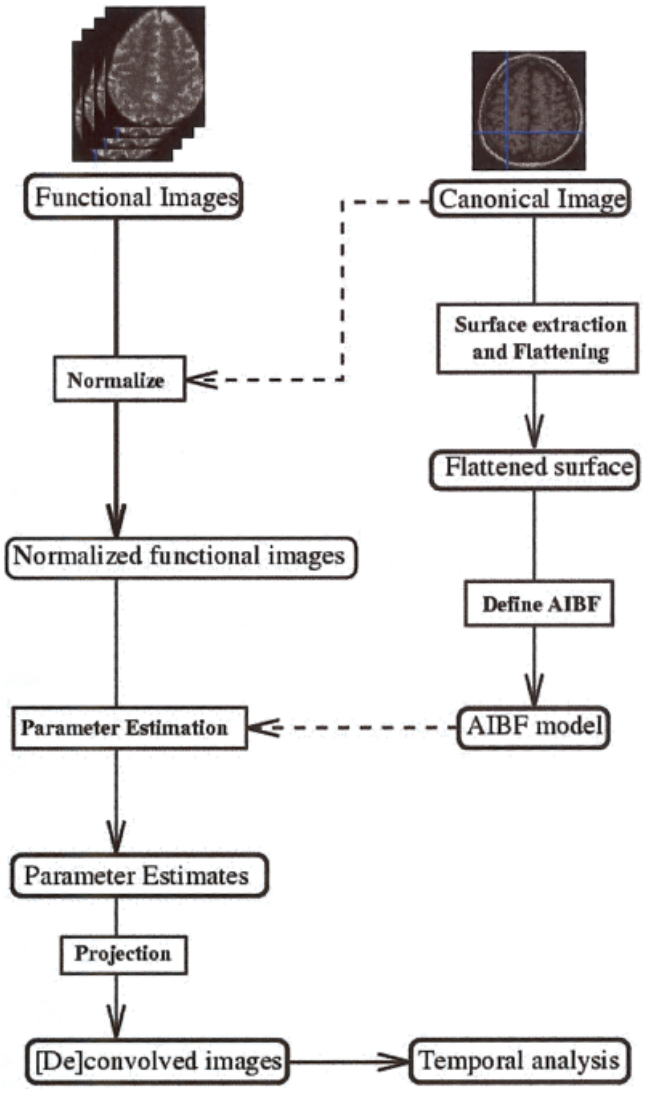

Figure 2.
Flowchart describing the data analysis stream in an AIBF-analysis from functional data and a canonical image to the temporal analysis of the projected images, i.e., source estimates. Solid arrows: transforms of data, dashed arrows: transfer of information. [Color figure can be viewed in the online issue, which is available at www.interscience.wiley.com.]

with a word that began with the letter presented (intrinsic word generation).

The functional data were realigned and spatially normalized using SPM99. Normalized images had a voxel size of 2 mm in each direction. A canonical grey matter surface of a normal brain was reconstructed using a T_1-weighted MRI sequence with voxel-sizes of $1 \times 1 \times 1$ mm. The subject providing the canonical surface came from the same population, but did not take part in the PET study. The MR sequence was optimized for grey-white contrast and is described in Deichmann and Turner [2000].

The analysis was constrained to a volume of interest (VOI), because a practical constraint of the AIBF approach is the inversion of a $N_P \times N_P$ matrix (equation 4) that limits the number of basis functions that can be used in the current implementation. This VOI encompassed the left frontal lobe. We chose Gaussian AIBFs with a width of 12 mm full width at half maximum (FWHM) and a separation of 12 mm. The kernel width of the Gaussian filter representing L_I was 8 mm and the width of L_E was 16 mm. These parameters gave 150 Gaussian basis functions covering the whole surface of the left frontal lobe. We also added a global basis function corresponding to the mean intensity of the spatially normalized image-series. After estimating the parameters, we projected B to A-space, i.e., to voxel-space, but discounting the effects of convolution with L_I and L_E. Finally, the projected images were analyzed in the time domain using SPM99, modelling condition- and subject-specific effects in the usual way.

For cross-validation we employed a conventional voxel-based univariate analysis using SPM99 based on a spherical and stationary smoothing kernel. We smoothed the same realigned and normalized images as used in the AIBF-analysis with an isotropic Gaussian kernel with a FWHM of 16 mm in each direction. We used the same model for temporal analysis.

fMRI data

Data from five right-handed subjects were analyzed, where each subject performed a finger opposition task. Subjects opposed the middle finger and thumb of the right hand at a self-paced frequency of 0.5 Hz. All subjects were right-handed. The functional data (EPI, gradient echo) were acquired on a clinical 1.5 T Siemens Vision unit (Siemens GmbH, Erlangen) with TR = 168 msec, TE = 79 msec, flip angle = 90°. Each image consisted of 128×128 voxels, 20 slices, transverse orientation, voxel size $1.8 \times 1.8 \times 3$ mm^3. For each subject, the position and orientation of the slices were chosen to cover all the brain volume superior to the corpus callosum, in particular the primary sensorimotor hand area.

Twenty-three scans were acquired and the first three scans were discarded to ensure steady state transverse magnetization. The design was blocked with a single activation epoch consisting of seven scans, starting at Scan 8.

The functional data were realigned and spatially normalized using SPM99. In this study, we used a subject's surface as canonical surface. We chose a VOI between the left frontal and left parietal lobe encompassing the left central sulcus. For the AIBF model, we used Gaussian basis functions with a width of 3 mm FWHM and a separation of 3 mm. L_I was chosen as the identity matrix and L_E corresponded to a Gaussian smoothing of [4 4 6] mm FWHM into x-, y- and z-direction. The estimated parameter matrix B was projected into A-space before proceeding with a conventional voxel-based analysis using SPM99. The statistical model (temporal basis functions) comprised a box car stimulus function convolved with a hemodynamic response function (HRF).

As with the PET analysis, a conventional voxel-based analysis was also performed using conventional stationary smoothing. The data were smoothed with a Gaussian kernel of [10 10 12] mm FWHM into x-, y- and z-direction. This specific smoothing filter was chosen to ensure that both AIBF and CS analyses resulted in approximately the same estimated smoothness of the components of the t-field. The same model was used to characterize the smoothed images in the time-domain.

RESULTS

PET multisubject study

The two resulting SPM{t} of the AIBF- and the conventional smoothing (CS) analysis are shown as maximum intensity projections (MIPs) in Figures 3 and 4. The t-maps were thresholded at $P < 0.01$ (corrected) and overlaid on an individual structural MRI. Both SPMs are centered on their maximum t-value. As it can be seen, the CS-SPM appears to be rather smooth, but interestingly both maps have approximately the same smoothness along the three coordinate axes. The CS-SPM has an estimated FWHM of [11.3 11.9 12.2] mm in x-, y- and z-direction, and the AIBF-SPM has a FWHM of [13.3 12.1 12.3]. These are averages over the entire volume based on the determinant of the covariances of the residual field gradients at each voxel. The relevant t-value maxima, P-value minima and their location for both analyses are shown in Tables I and II. The search volume of the CS-SPM was 42,501 voxels, whereas the AIBF-analysis comprised only 7,964 voxels. This discrepancy arises during the back-projection of the AIBF-parameter matrix B into A-space, i.e., the fitted data is deconvolved such that the search volume is reduced to the discretized grey matter partition. The resel count [Worsley et al., 1996a] for the AIBF-analysis was [−92 73.56 179.21 2.15] and [1 22.7 139.20 182.83] for the CS-analysis. These volume metrics can be thought of as volume estimates normalized by smoothness for 0, 1, 2, and 3 dimensions. It can be seen that the 2D resel count surpasses the 3D count for the AIBF-analysis in contradistinction to the CS-analysis. These analyses demonstrate the enhanced anatomical precision of the inferences that can be obtained using AIBF without impairing sensitivity.

fMRI multisubject study

The resulting MIPs centered on the maximum t-values of the AIBF- and CS-analysis are shown in Figures 3 and 4. The t-maps were thresholded at $P < 0.01$ (corrected) and overlaid on a structural MRI of a subject's brain. Each analysis detected an activation cluster around the hand knob in the left central sulcus. The peak t-value computed using the AIBF-analysis was 9.62, corresponding to a P-value of $6.00\ 10^{-10}$ and was located at [−43.8 −18.4 54.0]. The CS-analysis t-maximum was 7.89 ($P = 1.07\ 10^{-6}$), located at [−47.4 −20.2 60.0]. The estimated smoothness of the SPM{t} were similar. For the AIBF-analysis, it was [11.8 10.2 15.7] and for the CS-analysis [12.3 12.1 13.7]. The search volumes were 7,347 voxels (AIBF) and 32,329 voxels (CS). The resel count [Worsley et al., 1996a] for the AIBF-analysis was [−83 63.74 191.47 3.11] and [1 21.26 106.71 135.13] for the CS-analysis.

DISCUSSION

We have presented a new procedure to analyze multisubject neuroimaging data (fMRI, PET, SPECT). The method uses anatomically informed basis functions (AIBF) that are constrained by a canonical grey matter surface.

The estimation and the projection of the AIBF model parameters, as described in equations (6) and (9), implement a spatially variable or non-stationary smoothing that conforms to the cortical sheet. This smoothing is the only difference between the AIBF approach and a conventional analysis. All other processing steps (realignment, normalization, statistical modelling in the time-domain, statistical inference) are identical.

The AIBF [de]convolution approach projects the estimated parameters in AIBF-space back to the cortical sheet. Because this projection omits the spatial convolution operators in the forward model, it is effectively a deconvolution. This deconvolution can be regarded as solving the inverse problem to estimate the source

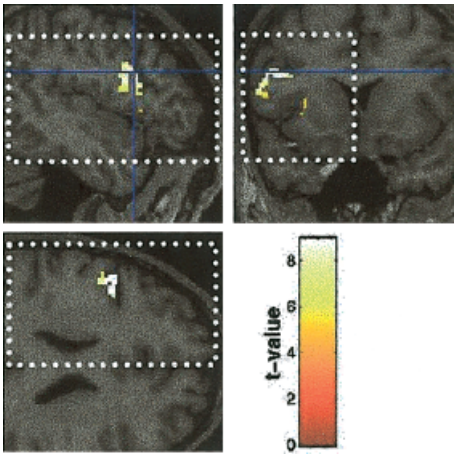

Figure 3.
AIBF results for PET data. t-Map thresholded at $P < 0.01$ (corrected) overlaid on the normalized structural MRI that was used for generating the canonical surface. The white dotted lines indicate the volume of interest analyzed.

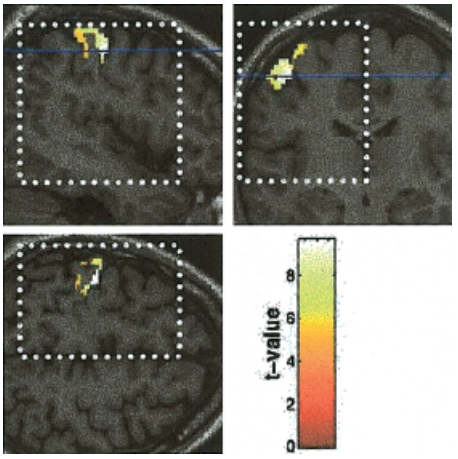

Figure 5.
AIBF results for fMRI data. t-Map thresholded at $P < 0.01$ (corrected) overlaid on the normalized structural MRI that was used for generating the canonical surface. The white dotted lines indicate the volume of interest analyzed.

distribution in PET or fMRI studies. The search volume after deconvolution is smaller than in a conventional analysis, in which the search volume covers not only the cortical sheet, but also the surrounding tissue. Decreasing the search volume reduces the adjustment to the *P*-values, provided the smaller search volume does not become too convoluted [Worsley et al., 1996a]. Another effect of the deconvolution is that inference is with respect to the sources on the cortical sheet enabling AIBF to provide more anatomical precision than conventional analyses. This assumes that all activations originate in or close to the cortical sheet. One can control the meaning of *close* by varying the width of the filter L_E (equations 2, 3).

An interesting aspect of our results is the difference in resel count between the AIBF- and CS-analyses, especially the discrepancy of the resel count in the 3rd dimension (2.15 vs. 182.83 in the PET study). This indicates that the AIBF-search volume resembles a surface rather than a volume. Note that an inflation of the surface resel term might cause an increase in the corrected *P*-values as discussed in Worsley et al.

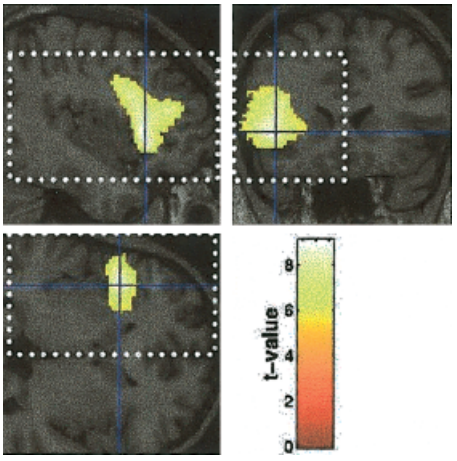

Figure 4.
CS results for PET data. t-Map thresholded at $P < 0.01$ (corrected) overlaid on the normalized structural MRI that was used for generating the canonical surface. The white dotted lines indicate the volume of interest analyzed.

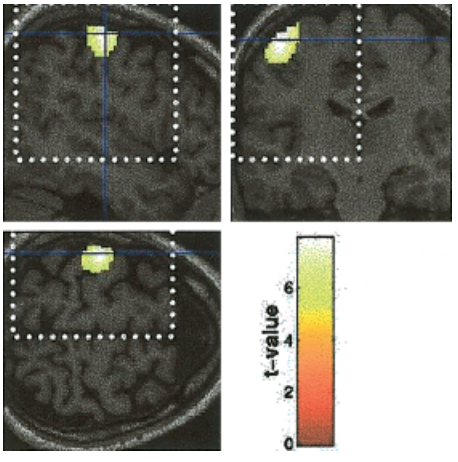

Figure 6.
CS results for fMRI data. t-Map thresholded at $P < 0.01$ (corrected) overlaid on the normalized structural MRI that was used for generating the canonical surface. The white dotted lines indicate the volume of interest analyzed.

TABLE I. AIBF-analysis: location, *t*-value and corrected *P*-value of maxima in activation clusters

Location	*t*-value	*P*-value
−48/12/24	8.92	5.8810^{-8}
−42/46/20	6.08	3.9610^{-4}
−32/20/2	5.90	6.9610^{-4}
−48/16/2	5.11	7.6010^{-3}

[1996a]. We did not, however, characterize the relationship between voxel-size and *P*-values explicitly.

There were some differences between the statistical results of AIBF and CS-analyses of the PET data. The CS-analysis found an apparently smoother representation of the underlying activation in the sense that the resulting SPM{t} showed one large highly significant *cluster*. In contrast to this, AIBF, although having roughly the same estimated average smoothness, provided a SPM{t} that showed distinct clusters (in 3D-space) that fell into locations similar to the maxima of the CS-SPM. This is in accord with the shape of the AIBF kernel, which is smooth tangential to the cortical sheet, but not orthogonal to the sheet. This feature provides higher anatomical precision by effectively removing spatial variability in the estimated sources that is orthogonal to the cortical surface.

With the fMRI data, both analyses found evidence for an activation in the left central sulcus close to the hand knob [Yousry et al., 1997]. There were two fundamental differences, however, between the AIBF- and CS-results. First, the *P*-value of the AIBF-analysis was smaller (more significant) than the corresponding minimum found using CS. This is most likely due to the fact that the activation induced by the finger tapping paradigm was distributed along the cortical surface within the central sulcus, over a distance of some mm. This activation pattern is properly modelled by smooth components along the cortical surface, enabling AIBF to detect the underlying activation. In contrast, a stationary smoothing filter is suboptimal in this situation, because it cannot follow the cortical surface. Second, the location identified by the AIBF-analysis (z-height 54 mm) was closer to the hand knob than the location indicated by the CS-analysis (z-height 60 mm). It is evident from Figure 6 that the location found by CS is rather lateral and inspection of the underlying single-subject results (data not shown) indicated that this cluster was due to activations within cerebrospinal fluid (CSF). This suggests that the activation estimated by AIBF is closer to the neuronal activation. This conclusion is based on the assumed anatomical-functional relationship of the hand knob in the anterior bank of the central sulcus and the primary motor area of the hand [Yousry et al., 1997].

As a caveat, note that the fMRI activation cluster has been mapped by AIBF to the posterior bank of the sulcus, although one would have expected some proportion of the activation to arise in the anterior bank, evoked by the motor components of the task. There was, however, some non-significant activation on the anterior bank. Inspection of the single subject SPMs showed that most individuals' activations were located within the central sulcus and not directly in the grey matter on either side. Another possible explanation for the location in the posterior bank is given by a potentially imperfect spatial normalization that misregistered the subjects' central sulci and their hand knobs. This was partially the case in our five data sets and speaks to the utility of a spatial normalization that explicitly incorporates surface-based information. The anatomical variability in brain regions other than the hand area, however, is probably higher than in first order areas [Amunts et al., 1999, 2000] and an improved landmark- or surface-based normalization would not necessarily improve the alignment of higher order functional areas.

Another question, related to the spatial normalization, is how one chooses a canonical surface. The basic assumption about the canonical surface is that it is a reasonable model of the subjects' cortical surfaces. The main requirement is that the spatially normalized (individuals') cortical surfaces and the canonical surface have roughly the same configuration. To moderate violations of this assumption, one can use the spatial lowpass filter L_E to trade resolution for model robustness. The primary advantage of the AIBF method, sensitivity for spatially extended activations tangential to the cortical surface, is compromised, however, if the canonical surface is substantially different from the actual surface. Therefore, before applying AIBF, one should verify that the canonical surface is a

TABLE II. CS-analysis: location, *t*-value and corrected *P*-value of maxima in activation clusters

Location	*t*-value	*P*-value
−40/20/0	9.05	2.4010^{-7}
−46/10/26	8.64	7.8710^{-7}
−38/34/16	8.28	2.3210^{-6}
−38/46/18	5.60	5.2010^{-3}

reasonable model of all the subjects' cortical surfaces.

Note that one should avoid a high ratio of the width of L_E and the Gaussian basis functions. This is because the smoothed basis functions in voxel-space A_L (equation 2) then become roughly overlapping. The ensuing parameters scaling the contribution of each basis function then become highly correlated and differences among them are estimated very inefficiently. The fit would not have much value for making an inference about the location of an activation.

This means that for multisubject studies real variations in function-structure relationships and structural variation due to imprecise spatial normalization set equivalent bands on the width of the AIBF. The relationship means that the registration in a multisubject study constrains the effective resolution of the inference.

Finally, we discuss AIBF in relation to the cortical surface mapping (CSM) approach [Andrade et al., 2001] that also takes the cortical surface into account to constrain the statistical analysis of functional data. In contradistinction to AIBF, which uses an explicit forward model, CSM uses an interpolation of the functional data to solve the inverse problem posed by dispersion of measured brain responses away from the cortical surface. This interpolation samples the functional voxel values of each image at each surface vertex on the cortical surface. Subsequently, the estimates of cortical activity are smoothed iteratively over the surface. The iterative smoothing is necessary, because the cortical surface consists of an irregular grid embedded in 3D-space. After the smoothing, the time-series at each vertex are analyzed with a standard data-sequence approach.

The theoretical basis of both methods are quite different. AIBF computes a forward model and solves the inverse problem of explaining the functional data by a distribution that is smooth tangential to the cortical surface. CSM does not use a forward model, but uses interpolation and smoothing to project fMRI data to the cortical surface. There follow some salient differences between CSM and AIBF. First, AIBF can project onto any space that was used in the forward model. One can project to the basis function space, the cortical surface space, or (as in this study) to voxel-space. With CSM, one projects to the cortical surface. Second, the forward model of AIBF can be adapted to any kind of neuroimaging data, for instance, to PET data [Kiebel et al., 2000]. Third, a multisubject approach as presented in this study is presently not possible with CSM. Andrade et al. [2001], however, discuss the possibility of using a surface normalization after the interpolation to enable a multisubject analysis. Fourth, the forward model of AIBF allows extensions like modelling explicitly structures on the cortical surface (e.g., thick/thin stripes in visual area V2). Another extension is the inclusion of draining veins in the forward model (identified by a venogram) to differentiate between signal intensities generated in veins or in grey matter locations. The veins would be modelled by 1D-basis functions embedded in 3D-space. Furthermore, AIBF can be incorporated into a proper Bayesian framework with priors on the parameters. This allows one to incorporate beliefs about the underlying distribution of the activations.

One final difference between the two methods is that CSM renders the smoothness across the cortical surface stationary, whereas using AIBF leads to a spatially variable smoothness due to the intrinsic distortions introduced during the flattening.

CONCLUSION

We have shown that anatomically informed basis functions (AIBF) can be used to analyze neuroimaging (fMRI and PET) multisubject data by using a canonical cortical surface. AIBF effectively implements a non-stationary, anatomically informed filter kernel that increases sensitivity to smooth activations confined to the cortical sheet. Critically the ensuing spatial [de]convolution is pre-defined and is the same for all functional data that are assumed to be generated by the same canonical surface. The AIBF filter can be chosen to implement a smoothing or deconvolution of the functional data by omitting any convolutions in the forward model. We have shown that the deconvolution approach leads to better anatomical precision and increases sensitivity, in relation to conventional analyses.

ACKNOWLEDGMENTS

SK and KJF were supported by the Wellcome Trust.

REFERENCES

Amunts K, Malikovic A, Mohlberg H, Schormann T, Zilles K (2000): Brodmann area 17 and 18 brought into stereotaxic space: where and how variable. Neuroimage 11:66–84.

Amunts K, Schleicher A, Burgel U, Mohlberg H, Uylings H, Zilles K (1999): Broca region revisited: cytoarchitecture and intersubject variability. J Comp Neurol 20:319–341.

Andrade A, Kerif F, Mangin JF, Worsley KJ, Paradis AL, Simon O, Dehaene S, Bihan DL, Poline JB (2001): Detection of fMRI acti-

vation using cortical surface mapping. Hum Brain Mapp 12:79–93.

Ashburner J, Friston K (1999): Nonlinear spatial normalization using basis functions. Hum Brain Mapp 7:254–266.

Collins D, Neelin P, Peters T, Evans A (1994): Automatic 3D intersubject registration of MR volumetric data in standardized Talairach space. J Comput Assist Tomogr 18:192–205.

Deichmann R, Turner R (2000): Optimization of 3D MP-RAGE sequence for structural brain imaging. Neuroimage 12:112–127.

Dempster A, Laird N, Rubin D (1977): Maximum likelihood from incomplete data via the EM algorithm. J R Stat Soc [Ser B] 39:138.

Fischl B, Sereno MI, Dale AM (1999): Cortical surface-based analysis, II: Inflation, flattening, and a surface-based coordinate system. Neuroimage 9:195–207.

Friston K, Holmes A, Price C, Buechel C, Worsley K (1999): Multisubject fMRI studies and conjunction analyses. Neuroimage 10: 385–396.

Kiebel S (2001): Anatomically informed basis functions. PhD thesis, Otto-von-Guericke, Universität Magdeburg.

Kiebel S, Goebel R, Friston K (2000): Anatomically informed basis functions. Neuroimage 11:656–667.

Poline JB, Mazoyer B (1994): Enhanced detection in brain activation maps using a multifiltering approach. J Cereb Blood Flow Metab 14:639–642.

Press WH, Teukolsky SA, Vetterling WT (1992): Numerical recipes in C: the art of scientific computing. Cambridge: Cambridge University Press. p 808–813.

Talairach J, Tournoux P (1988): Coplanar stereotaxic atlas of the human brain. New York: Thieme Medical.

Worsley K, Marrett S, Neelin P, Vandal A, Friston K, Evans A (1996a): Searching scale space for activation in PET images. Hum Brain Mapp 4:74–90.

Worsley KJ, Friston KJ (2000): A test for a conjunction. Statistics and Probability Letters 47:135–140.

Worsley KJ, Marrett S, Neelin P, Vandal A, Friston K, Evans A (1996b): A unified statistical approach for determining significant signals in images of cerebral activation. Hum Brain Mapp 4:58–73.

Yousry TA, Schmid UD, Alkadhi H, Schmidt D, Peraud A, Buettner A, Winkler P (1997): Localization of the motor hand area to a knob on the precentral gyrus. Brain 120:141–157.